Pakistan Veterinary Journal

ISSN: 0253-8318 (PRINT), 2074-7764 (ONLINE)
DOI: 10.29261/pakvetj/2026.118

RESEARCH ARTICLE

Tupistra chinensis Polysaccharide Strengthened Immunity in Mice Induced by Cyclophosphamide Via Regulating Microbiota

Qing He[1], Xinru Wang[1,2], Tao Luo[1,3,4], Hadil Alkathiry[5], Manal Abduallah Alduwish[6], Mahmoud M. Abdelwahab[7], Wentong Liu[2]*, Huijuan Sun[3]* and Quzhen Deji[4]*

[1]College of Veterinary Medicine, Nanjing Agricultural University, Nanjing 210095, China; [2]School of Basic Medicine, Hubei University of Arts and Science, Xiangyang 441000, China; [3]Innovation Center for Edible Fungi Resources and Application Technology, Xizang Autonomous Region, Lhasa 850000, China; [4]Institute of Animal Husbandry and Veterinary Medicine, Xizang Academy of Agricultural and Animal Husbandry Sciences, Lhasa 850009, China; [5]Department of Biology, College of Science, Imam Mohammad Ibn Saud Islamic University (IMSIU), Riyadh, Saudi Arabia; [6]Department of Biology, College of Science and Humanities in Al-Kharj, Prince Sattam Bin Abdulaziz University, Alkarj 11942, Saudi Arabia; [7]Department of Mathematics and Statistics, Faculty of Science, Imam Mohammad Ibn Saud Islamic University (IMSIU), Riyadh 11432, Saudi Arabia.
*Corresponding author: 11847@hbuas.edu.cn (WL); m18898002012@163.com (HS); quzhen@taaas.org (QD).

ARTICLE HISTORY (26-280)

Received: March 27, 2026
Revised: April 26, 2026
Accepted: April 28, 2026
Published online: April 30, 2026

Key words:
Cyclophosphamide
Gut microbiota
Immune function
Tupistra chinensis polysaccharide

ABSTRACT

The effect of *Tupistra chinensis* polysaccharide on the immunity and microbiota of mice induced by cyclophosphamide (CTX) in mice was investigated. In total, forty ICR mice aged about 4 weeks were randomly divided into 4 groups (n=10/group) with blank control group (CCAR), immune deficiency model group (MCAR), positive control group (LHAR), and *Tupistra chinensis* polysaccharide group (PCAR). Mice in the MCAR, LHAR, and PCAR groups received intraperitoneal injections of CTX for 3 consecutive days. Additionally, from the fourth day, 0.2mL of normal saline was given to mice in the CCAR and MCAR groups, while 40mg/kg of levamisole (LH) was administered to mice in the LHAR group daily; likewise, mice in the PCAR group were given 100mg/kg *Tupistra chinensis* polysaccharide (TCP) every day, for 14 days. Serum biochemistry, H&E staining, and gut microbiome sequencing indicated that TCP significantly alleviated CTX-induced immune dysfunction. Malondialdehyde levels in the TCP-treated group were lower than those in the model group. In contrast, interleukin *(IL)-6*, *tumor necrosis factor-alpha, IL-1 beta, IL-10*, total antioxidant capacity, and superoxide dismutase levels were higher in the TCP-treated group compared to the model group. The sequencing data showed that TCP supplementation restored the intestinal microbiome and its function in mice with CTX-induced changes. TCP down-regulated the abundance of noxious microbes, such as *Dwaynesavagella, Streptococcus,* and *Duncaniella*, and there was an increase in the beneficial bacteria like *Limosilactobacillus* and *Ligilactobacillus* in the gut. It was concluded that TCP has a restorative effect on CTX-induced immune dysfunction in mice by regulating oxidative stress and restoring the intestinal microbiome.

To Cite This Article: He Q, Wang X, Luo T, Alkathiry H, Alduwish MH, Abdelwahab MM, Liu W, Sun H and Deji Q, 2026. *Tupistra chinensis* polysaccharide strengthened immunity in mice induced by cyclophosphamide via regulating microbiota. Pak Vet J, 46(5): 1313-1323. http://dx.doi.org/10.29261/pakvetj/2026.118

INTRODUCTION

The immune system is capable of identifying and eliminating invading pathogens, their toxins, and tumor cells resulting from genetic mutations. This process provides immune defense and helps in maintaining the body's homeostasis (Meng *et al.,* 2024). Maintaining normal immune function is vital for the stability of the body (Peng *et al.,* 2024). Cyclophosphamide (CTX) is a commonly used immunosuppressant that exerts its effects by inhibiting DNA synthesis, which hinders lymphocyte proliferation (de Jonge *et al.,* 2005). CTX can be used in the clinical treatment of malignant lymphoma, acute or chronic lymphocytic leukemia, and autoimmune diseases (Ponticelli & Glassock, 2019; Kara, 2024). LH is a common immune booster, which was used to treat rheumatoid

arthritis and some cancers because of its immunomodulatory properties (Cascio & Jen, 2018).

The gut microbiota in the host's gastrointestinal tract (GIT) functions as a highly active "hidden organ" that is involved in numerous defense mechanisms and plays critical roles in physiological activity during health and disease conditions (Nguyen *et al.,* 2024; Xu *et al.,* 2025). Statistics indicate that a normal gut contains more than 10^{14} microbes, which are about 10 times the total number of host cells (Shim, 2013; Wang *et al.,* 2024) Although it has long been assumed that microbial cells outnumber human cells by approximately ten to one, more recent and detailed analyses suggest that the ratio is closer to 1:1, with variation depending on factors such as individual body size and the amount of fecal material in the colon (Sender *et al.,* 2016; Rosshart *et al.,* 2023). Gut bacteria constitute about 98% of the total microbiome, with the rest including fungi, *viruses,* and protozoa (Dong *et al.,* 2019; Lin *et al.,* 2023). In addition to bacteria, fungi, viruses, and protozoa, archaea also constitute an important component of the gut microbiome, contributing to key processes such as methanogenesis and host energy metabolism. Beneficial intestinal bacteria restrict the colonization of foreign pathogens by secreting antimicrobial peptides, regulating the intestinal environment, and competing for nutrients. This combined activity serves as a natural barrier against the pathogens' invasion (Biswas *et al.,* 2012; Huang *et al.,* 2021). The gut microbiota regulates the immune system by producing molecules with immunomodulatory functions, which can regulate the response of immune cells, including lymphocytes, etc (Cai *et al.,* 2023; Zheng *et al.,* 2023). Disruptions in gut flora have been linked to immune disorders, including inflammatory bowel disease, rheumatism, thyroid disease, and asthma (Zhang *et al.,* 2018; Ahlawat *et al.,* 2021; Virili *et al.,* 2021).

Tupistra chinensis, commonly also known as Yanqi, Dahan medicine, bamboo root ginseng, or oxtail seven, belongs to the Liliaceae family of Convallarieae genus (Xiao *et al.,* 2019; Li *et al.,* 2024). *Tupistra chinensis* grows in southwest China and has dry roots that are used as a folk medicine in the *Shennongjia Forestry District*, a National Nature Reserve in Hubei. This is renowned for its effectiveness in significantly reducing swelling and soothing the throat (Pan *et al.,* 2000). This Chinese herb is usually employed to treat throat irritation, rheumatism, dermatomyositis, and snake bites (Pan *et al.,* 2012; Xu *et al.,* 2020). The extract of *Tupistra chinensis* has been found to be an apoptosis-inducing agent and possesses autophagy activities with few side effects (Yi *et al.,* 2018). Immune-related diseases are frequently observed in livestock and poultry, yet there are limited effective treatments available using Chinese herbal medicine. Over the past decade, phytochemical studies of *Tupistra chinensis* have identified several steroidal sapogenins and non-steroidal saponins with potential therapeutic value (Wei *et al.,* 2014); to find new bioactive metabolites from this herb to regulate immune function, polysaccharides were isolated from its rhizomes. The results of modern pharmacological experiments have shown that polysaccharides have many bioactivities, like immune adjustment, anti-microbial activity, anti-cancer, and anti-virus (Ying *et al.,* 2024). The relative molecular mass of polysaccharides is 1831–1910 Da, the coefficient of their MW distribution is around 1.31 to 1.35, and the purity of polysaccharides is 80% (Zhang *et al.,* 2018).

Limited information is available on the effects of *Tupistra chinensis* polysaccharide on cyclophosphamide-induced microbiota in mice. Therefore, the present study was conducted to investigate the potential alleviating effect of *Tupistra chinensis* polysaccharide on the immune dysfunction caused by cyclophosphamide in mice.

MATERIALS AND METHODS

The extraction of Tupistra chinensis polysaccharide: The extraction was conducted following the established extraction methods for similar herbs (Zhang *et al.,* 2018). The optimal static and dynamic extraction continuances were one and a half hours, respectively. Briefly, *Tupistra chinensis* rhizomes (50.0kg) were washed and chopped, then defatted three times with 95% ethanol at 65°C. The remaining resin was extracted with three times hot water, concentrated, and dried to obtain crude polysaccharide. The yield was calculated based on the dry weight of crude polysaccharides and the dry weight of the medicinal raw materials and it was approximately 50.38% (w/w). These polysaccharides were precipitated with different ethanol concentrations viz; 30, 50 and 80%, respectively and then centrifuged at 2500rpm for 15 minutes. Following dialysis and decolorization, the bottom of the tube was converged and the three polysaccharides were named TCP-A, TCP-B, and TCP-C. We used the mixture of three *Tupistra chinensis* polysaccharides in subsequent experiments to explore its effects on GIT microbes.

Animals and experimental design: In total, forty ICR mice aged about 4-weeks with an average body weight of 22±1.5g of either sex, as approved by the ethics committee of Nanjing Agricultural University (NJAU. No. 20240226021). All mice were randomly divided into 4 groups: blank control group (CCAR), immune deficiency model group (MCAR), positive control group (LHAR), and *Tupistra chinensis* polysaccharide group (PCAR). Mice were acclimated for a week and fed freely in the laboratory, and then grouped and weighed. Except for the blank control group (CCAR), the other mice were injected I/P CTX 80mg/kg consecutively on the 3rd and 5th days (Zhao *et al.,* 2024). From the 4th day, the mice in group CCAR and group MCAR were given 0.2mL of normal saline daily, the positive control group (LHAR) was given 40mg/kg of levamisole (LH) daily, and the polysaccharide group (PCAR) was given 100mg/kg of polysaccharide daily according to the previous studies (Liang *et al.,* 2025).

After 14 days of continuous administration, the mice were euthanized (24 hours later by CO_2 inhalation and fasting), weighed, and blood samples were collected from the orbit after anesthesia. Additionally, the fecal samples were collected for serum and microbial quantitative analysis.

Serum biochemical, antioxidants and cytokine analysis: The collected blood samples from the four mice groups were subjected to centrifugation at 3000×g for 25 minutes to attain serum and were stored at -80°C for later use. The commercial detection kits were used to examine the contents of superoxide dismutase (SOD) and

malondialdehyde (MDA). Moreover, cytokines of interleukin 6 (IL-6), interleukin 10 (IL-10), IL-1β and TNF-α were detected via kits from the same company following the manufacturer's instructions.

Intestinal microbiome sequencing of mice: Total genomic DNA (n = 6 per group) from rectal contents of ICR mice was extracted using a commercial Stool DNA Isolation Kit (Aipudishengwu, China), and DNA was quantified by Nanodrop 2000 (Thermo Scientific, USA). The quality of DNA products in ICR mice was detected by 1.2% agarose gel electrophoresis. Subsequently, following previous studies, different regions of the 16S rRNA gene V3-V4 were amplified by PCR using specific primers (338F/806R). For purification and recovery, magnetic beads, magnetic bead washing solution, ethanol, and Elution Buffer were added to the amplified products. Fluorescence quantification of the recovered products by PCR amplification was carried out via Quant-iT PicoGreen dsDNA Assay Kit (BioTek, FLx800, USA). The sequencing Library was intended via the Illumina Library Prep Kit for double-ended sequencing via the MiSeq platform (Illumina, USA).

Histopathological analysis: Tissues from intestinal segments, jejunum, ileum, and colon, and the spleen of each mouse were harvested for histological evaluation. These tissues were fixed in 4% paraformaldehyde (4% PFA) over the next 48 h to preserve cellular structures and degradation. After marking fixation, the samples were paraffin-embedded for further sectioning. Thin sections (thickness: 4-5μM) were prepared and stained with hematoxylin and eosin (H&E), which is a routine method for examining tissue morphology. The stained sections were then assessed under a light microscope to determine the histopathological changes and structural integrity. Quantitative morphological analysis was conducted on the ileal tissue to evaluate its structural changes. The specific measured parameters include villus height and crypt depth, and the ratio of villus height to crypt depth (V/C ratio) was calculated. All measurements were performed on HE-stained tissue sections. For each experimental animal, three representative consecutive sections with an interval of approximately 100μM were selected. Under an optical microscope, five structurally intact and vertically oriented villus-crypt units were randomly selected from each section for measurement. To eliminate subjective biases, all measurement processes were completed by researchers who were unaware of the grouping information under single-blind conditions. The measurement was carried out using the ImageJ software. Firstly, the slice images were calibrated in scale. Then, the vertical distance from the top of the villi to the crypt opening (villi height) and from the crypt opening to the base (crypt depth) were manually measured using the straight-line tool in the software. The software automatically recorded the values in micrometers, and the V/C ratio was calculated.

Bioinformatics analysis of the mouse microbiome: Initially, the original data were qualitatively controlled, de-noised, spliced, and de-chimerized by the DADA2 method to generate feature sequences (ASVs) and then the current ASV sequences were compared with the green genes database for species annotation to generate a classification table. Differential abundance analysis was conducted using the LEfSe algorithm, with linear discriminant analysis (LDA) scores>2.0 and $P<0.05$ considered indicative of significantly different taxa between groups. Before performing LEfSe analysis, the data were normalized using relative abundance transformation at the taxonomic level of interest to account for differences in sequencing depth across samples. Before conducting LEfSe analysis to identify the differential microbial groups between groups, we divided the original count of each ASV in each sample by the total sequencing reading of that sample, thereby converting the data into relative abundance. This conversion is carried out directly at the most basic ASV level. This standardization process generated an abundance table with the sum of all samples being 1, which was subsequently used for LEfSe analysis. Additionally, analysis of similarities was used to analyze or draw sparse curves to evaluate the current sequencing depth, and microbiota diversity analysis of the four groups was carried out by examining alpha-diversity indexes and beta-diversity metrics. Alpha diversity was evaluated by Shannon index, Chao1 index, Faith index, Simpson index, and observed; beta diversity was analyzed by PCoA and NMDS using Bray-Curtis distance, and the differences between groups were tested by PERMANOVA. Subsequently, a Venn Diagram and LEfSe analysis were used to reveal the changes in microbiota between the four groups of mice. Analysis of differences in the bacterial communities at each level among different groups was conducted using multiple t-tests. PICRUSt2 can predict 16S rRNA gene sequences in multiple functional databases. By default, we provide the most commonly used annotations from MetaCyc, KEGG, and COG databases. At the same time, it can also use the 18S rRNA gene and ITS gene sequences to predict metabolic pathways in the MetaCyc database.

Statistical analysis: The experimental data were analyzed using GraphPad Prism 10.1.2 and one-way ANOVA. The results were expressed as mean ± standard error (mean ± SEM). To control the false positive results that may occur due to multiple hypothesis tests, the p-values were adjusted using the Bonferroni correction method and were observed statistically significant at $P<0.05$.

RESULTS

TCP treatment mitigated immune dysfunction caused by CTX: The results indicated that rabbit skin polysaccharide (TCP) could effectively alleviate the immune dysfunction in mice caused by cyclophosphamide (CTX). Analysis of H&E staining sections showed significant differences between groups. Histopathological examination revealed that the ileal sections of the MCAR group showed intestinal villi shedding (black arrow), vacuolar infiltration of the upper mucosa (red arrow), and collagen fiber hyperplasia (green arrow). After LH or TCP treatment, the above-mentioned lesions decreased. Interestingly, in the LHAR group, there was still collagen fiber hyperplasia (green arrow) and some loss of small intestinal villi (black arrow), while the recovery degree of the above lesions was greater after

TCP treatment (Fig. 1a). Similarly, in the colon sections, the MCAR group showed mild structural abnormalities of the colon, with the shedding of mucosal epithelial cells (black arrow), a small amount of inflammatory cell infiltration (red arrow), and mild submucosal edema of the tissue (green arrow). The colonic structure in the LHAR group remained abnormal, with epithelial cells shedding (black arrow), while the overall structure in the PCAR group was normal (Fig. 1b). In addition, on the splenic tissue sections, compared with the blank control group, the distinction between the white pulp and the red pulp in the MCAR group was unclear, the structure of the white pulp was not obvious, and the splenic nodules were not obvious. A large number of extramedullary hematopoietic cells can be seen in the red medullary (indicated by black arrows), accompanied by obvious proliferation of macrophages (indicated by red arrows). After LH treatment, the lesion improved somewhat, but the extramedullary hematopoietic cells still protruded (indicated by the black arrow), and the recovery was not as complete as that of the tcp treatment group (Fig. 1c). After levamisole infection, the height of intestinal villi in mice decreased significantly, and the V/C ratio decreased significantly ($P<0.05$). The depth of the crypts increased significantly ($P<0.05$). After the addition of oral arrow polysaccharides, the V/C ratio increased significantly, and the depth of the crypts decreased significantly ($P<0.05$, Fig. 2).

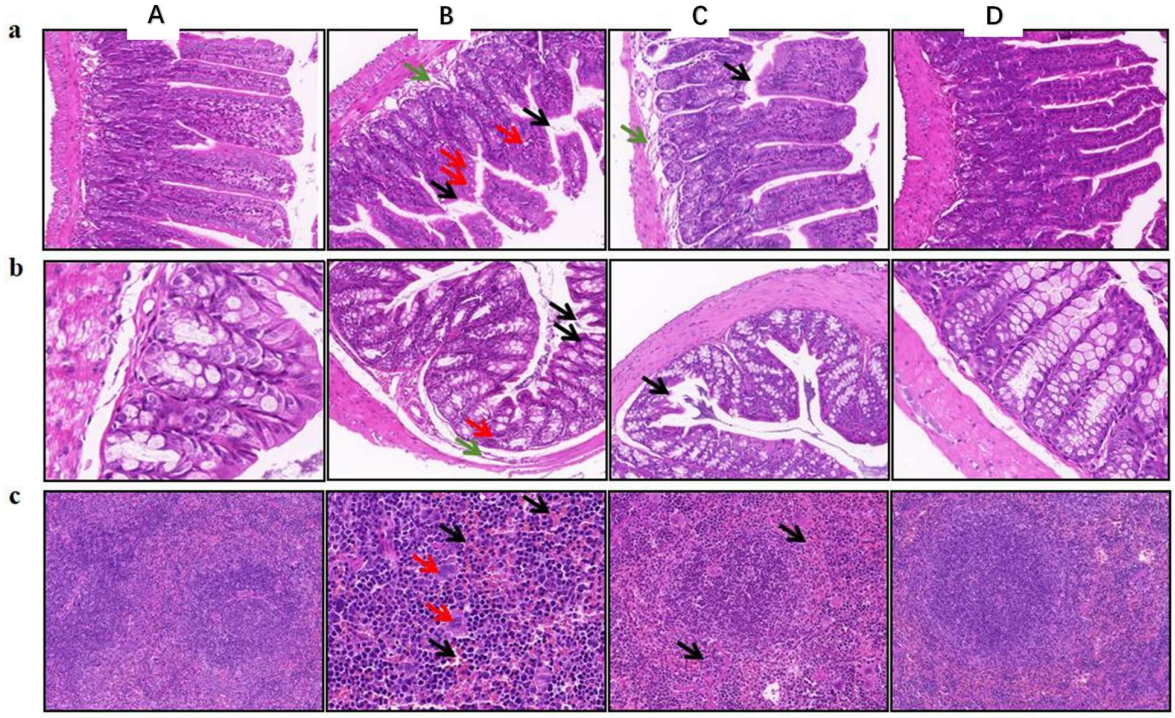

Fig. 1: *Tupistra chinensis* polysaccharide ameliorated immune system damage by cyclophosphamide in mice. a: Ileum, b: colon, c: spleen; A (Negative Control), B (cyclophosphamide treated group only), C (LH treated group after cyclophosphamide treated), D (TCP treated group after cyclophosphamide treated).

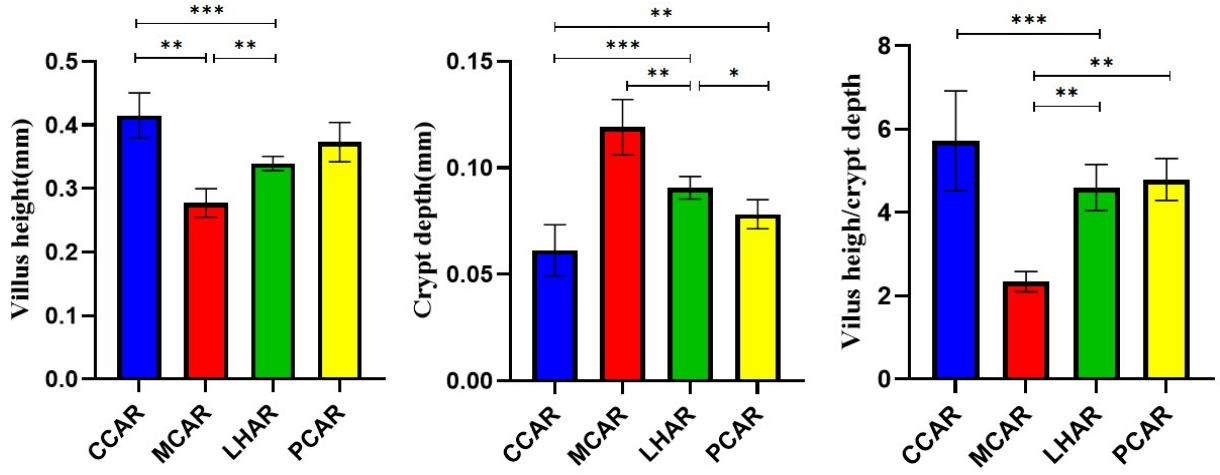

Fig. 2: The effect of *Tupistra* chinensis polysaccharide on villus height, crypt depth, and the villus height-to-crypt depth ratio of the ileum of mice. *P<0.05; **P<0.01; ***P<0.001.

Effects of TCP on cytokine levels, antioxidative activity, and serum biochemistry in mice: TCP significantly (P<0.05) improved cytokine levels, enhanced antioxidative activity, and positively influenced serum biochemistry indices in CTX-treated mice. In the MCAR group of CTX-induced ICR mice, serum concentrations of IL-6 and TNF-α were significantly reduced (P<0.05), with non-significant decreases observed in IL-1β, IL-10, and SOD levels. However, in the TCP treatment group, these markers of TNF-α showed significant increases, particularly IL-1β, which exhibited significant (P<0.05) elevation. Despite this improvement, the levels of these indices in the TCP group remained slightly lower or comparable to those in the LH treatment group (Fig. 3a-d, g). In the MCAR group, MDA concentrations exhibited a significant increase (P<0.05). Notably, following treatment with LH and TCP, there was a significant reduction in MDA levels (P<0.05); however, the decrease was slightly more pronounced in the PCAR group (Fig. 3e). The level of total antioxidant capacity (T-AOC) in the MCAR group was significantly decreased (P<0.05). Following treatment with LH and TCP, T-AOC levels were significantly (P<0.05) elevated; however, the T-AOC level in the LHAR group was marginally higher than that observed in the PCAR group (Fig. 3f). It was evident that the SOD level in the PCAR group was higher than that in the MCAR group, but not significant (Fig. 3g).

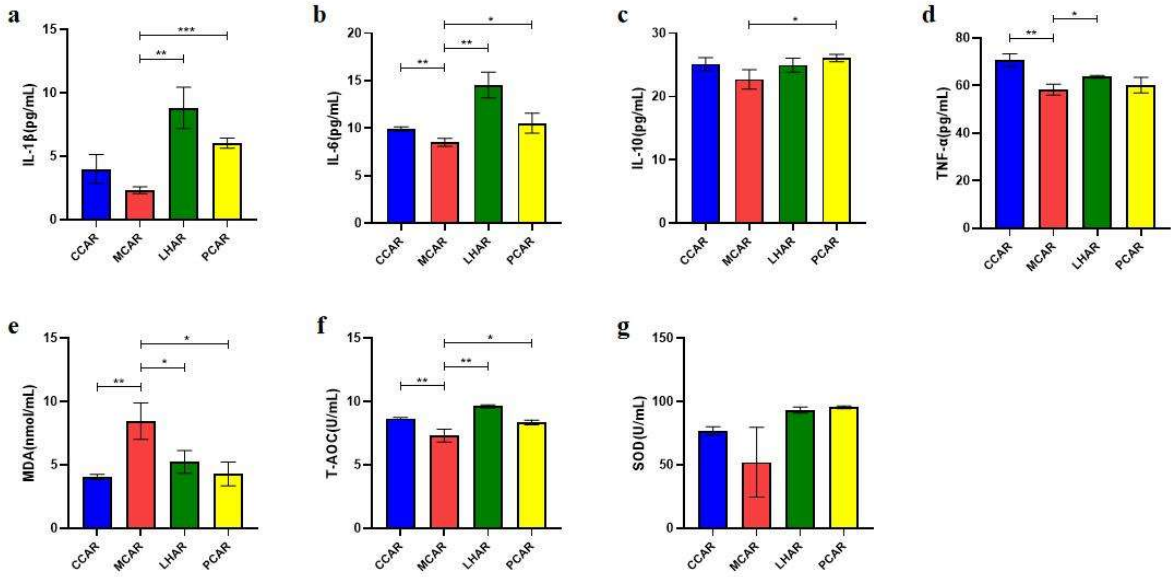

Fig. 3: The effect of *Tupistra chinensis* polysaccharide on cytokines and antioxidant abilities, and biochemistry indexes: (a) IL-1β, (b) IL-6, (c) IL-10, (d) TNF-α, (e) MDA, (f) T-AOC, (g) SOD. *P<0.05, **P<0.01, ***P<0.001; data were presented as the mean ± SEM.

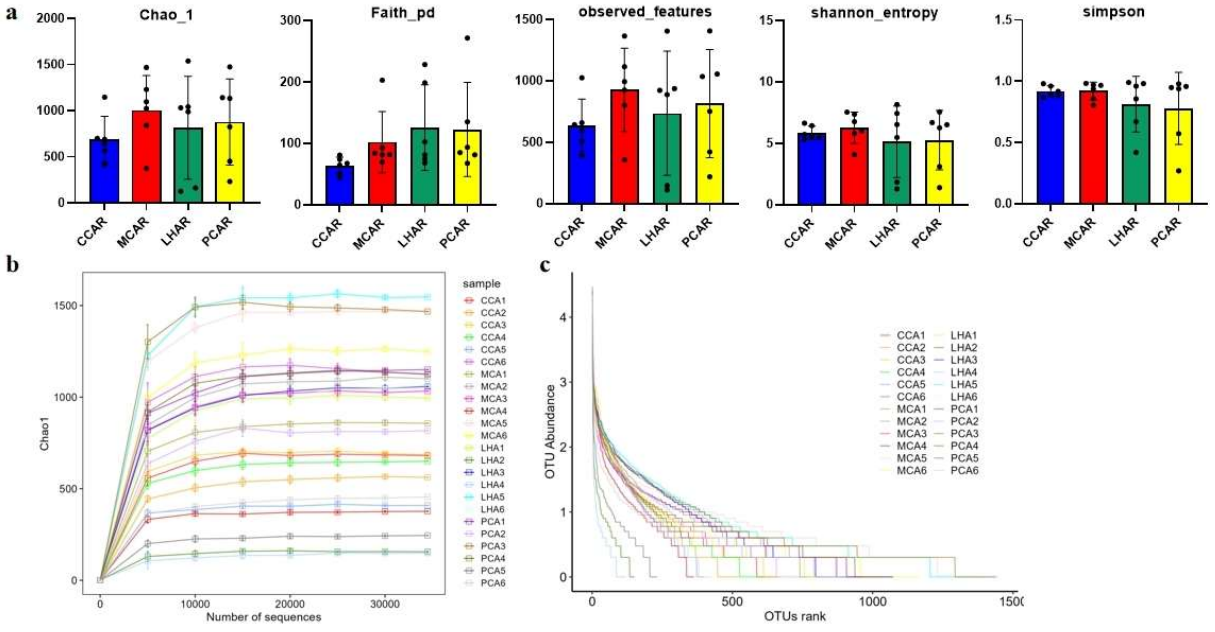

Fig. 4: The effect of *Tupistra chinensis* polysaccharide on alpha diversity indexes of the mouse microbiome. a: indexes, b: rarefaction curve, c: rank abundance curve.

TCP mediated microbiota in ICR mice: Except for the first error in the PCAR group, the filtering data of all groups of mice exceeded 91%. No obvious difference of alpha diversity among the mice groups was found (Fig. 4a). The sparse curve analysis showed that the Chao_1 value of the four groups tended to be flat under the same sequencing depth, and the model group (MCAR) had the least species (Fig. 4b). Except for the model group (MCAR), the abundance grade curves of all groups were relatively flat and had little difference, indicating uniform community composition between groups (Fig. 4c).

Venn map showed that there were 134 shared ASVs among the four groups, while there were 149, 151 and 146 shared ASVs between group CCAR and group MCAR, group LHAR and group PCAR, respectively (Fig. 5a). At the phylum level, *Firmicutes_D* (37.43%) and *Bacteroidota* (50.28%) were the main phyla of CCAR group, while *Bacteroidota*, *Firmicutes_D*, *Firmicutes_A* and *Campyloota* were the dominating phyla of group MCAR (28.44, 21.60, 29.67 and 11.26%), group LHAR (26.06, 26.76, 13.94 and 25.64%) and group PCAR (23.78, 19.06, 20.61 and 29.28%), respectively (Fig. 5b). At the class level, *Bacilli* (37.43%) and *Bacteroidia* (50.28%) were the most abundant classes in group CCAR, while *Bacilli*, *Bacteroidia*, *Clostridia_258483* and *Campylobacteria* were the stable classes in group MCAR (28.44, 21.60, 29.67 and 11.26%), group LHAR (26.06, 26.76, 13.94 and 25.64%) and group PCAR (23.78, 19.06, 20.61 and 29.28%), respectively (Fig. 5c). At the order level, *Lactobacillales* (35.49%) and *Bacteroidales* (50.14%) were dominant in the CCAR group, the main orders in MCAR group (23.39, 21.30, 22.73 and 11.26%) and PCAR group (21.72, 18.75, 14.60 and 29.29%) were *bacillales*, *Bacteroidales*, *Lachnospirales* and *Campylobacterales*, respectively, while the LHAR group were *Lactobacillales* (17.21%), *Bacteroidales* (26.12%) and *Campylobacterales* (25.65%) (Fig. 5d). At the family level, *Lactobacillaceae* (34.96%) and *Muribaculaceae* (35.68%) were dominant in the CCAR group, *Lactobacillaceae*, *Muribaculaceae*, *Lachnospiraceae* and *Helicobacteraceae* were the prime families in group MCAR (17.92,16.25, 22.76 and 11.27%) and PCAR (20.91, 14.51, 14.59 and 29.31%), while the three most abundant families in group LHAR were *Lactobacillaceae* (16.98%), *Muribaculaceae* (19.25%) and *Helicobacteraceae* (25.65%) (Fig. 5e). At the genus level, the main genera were *Lactobacillus* (27.71%), *Paramuribaculum* (10.57%) and *Duncaniella* (11.91%) in group CCAR, the main genera of group LHAR were *Lactobacillus* (13.97%), *Helicobacter_D* (12.87%) and *Helicobacter_C_479931* (13.05%), group PCAR were *Lactobacillus* (12.29%) and *Helicobacter_D* (26.82%), while the main genera of MCAR group was *Lactobacillus* (16.71%) (Fig. 5f).

Analysis of microbial diversity and composition in TCP-treated mice following CTX exposure: The analysis of the Beta-diversity index revealed that there was no prominent difference among the four groups (Fig. 6). However, PCA analysis showed that the distance between the MCAR group and other groups was slightly longer (Fig. 6a), non-metric multidimensional scale (NMDS) analysis reflected the relationship between microbial communities in different samples (Fig. 6b), and the microbial community structure of the blank control group and the model group was slightly different. The PERMANOVA analysis based on Bray-Curtis distance indicated that the differences in microbial community structures among the four groups did not reach statistical significance (pseudo $F = 1.145$, $p = 0.089$, $R^2 = 0.146$, 999 permutations test). The similarity among different groups was analyzed by UPGMA clustering (Fig. 6c). The results showed that there were significant differences in the main species between the MCAR group and other groups, and the number of main species was fewer. In addition, the distance between the TCP treatment group and group CCAR was smaller than between group CCAR and group MCAR.

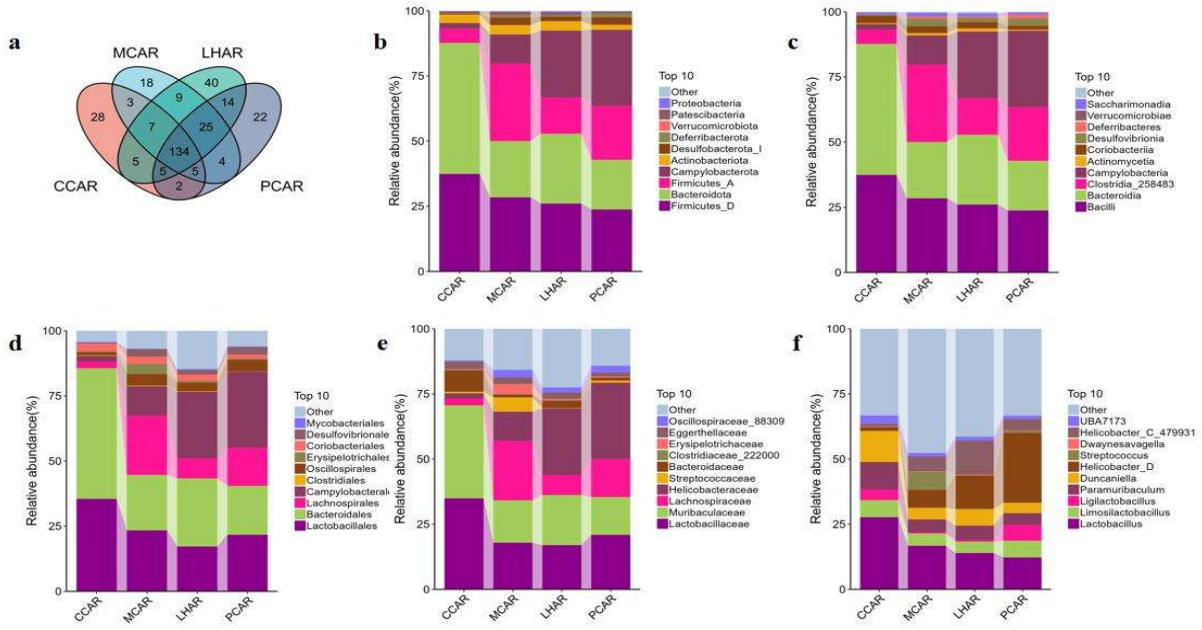

Fig. 5: The effect of *Tupistra chinensis* polysaccharide on intestinal microbiome composition of mice induced by cyclophosphamide by clustering heat map. a: Phylum, b: Class, c: Order, d: Family, e: Genus.

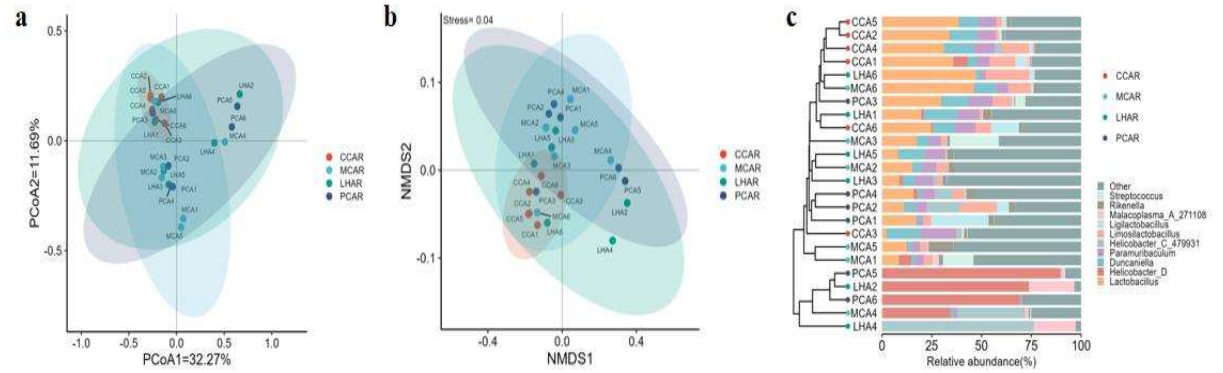

Fig. 6: Beta diversity analysis of mice. a: PCoA, b: NMDS, c: UPGMA.

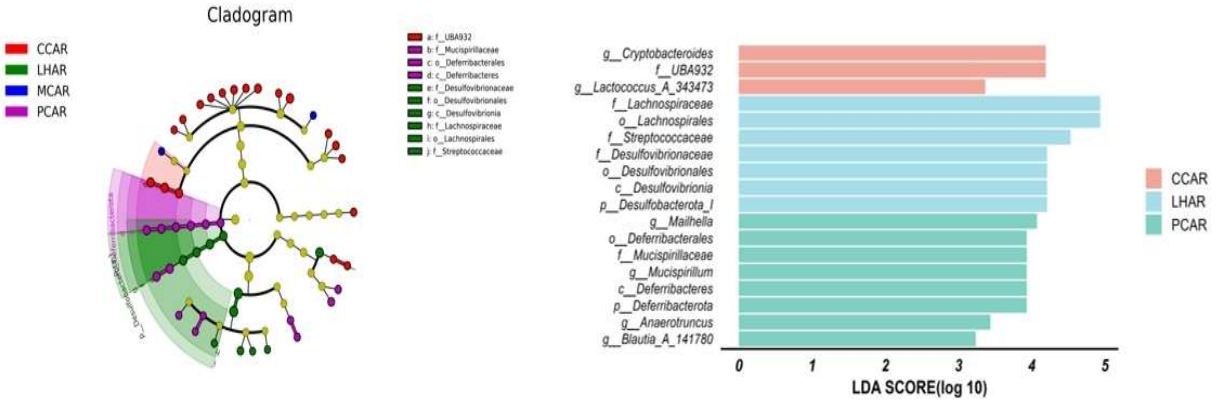

Fig. 7: Revealing the markedly different species between different groups via LEfSe.

LEfSe analysis revealed that there was non-significant difference in species between the MCAR group and other groups, the species abundance of the LHAR group and PCAR group was higher than that of the CCAR group, and the difference of LHAR group was the most significant (Fig. 7). The intestinal flora of normal mice was mainly *UBA932* (family level), *Cryptobacteroides* and *Lactococcus_A_343473* (genus level), mice in LH treatment group were *Lachnospiraceae*, *Desulfovibrionaceae*, *Streptococcaceae* (family level) and *Desulfovibrionia*, *Lachnospirales* (order level), mice in TCP treatment group were *Mucispirillaceae* (family level), *Deferribacterales* (order level) and *Deferribacteraes* (class level).

Through multiple T-tests, the differences in bacteria among various groups at different levels were analyzed. At the phylum level, the relative abundance of Deferribacterota in the PCAR group was significantly higher than that in the CCAR group (P=0.0302, Fig. 8a). At the genus level, the level of Cryptobacteroides in the PCAR group was significantly lower, while Mucispirillum (P=0.0247) and CAG-95 (P=0.0435) were significantly higher than the CCAR group (Fig. 8b). At the species level, compared with the CCAR group, the relative abundances of Duncaniella (P=0.0429) and Paramuribaculum sp000431155 (P=0.0014) in the MCAR group, UBA7173 sp900540205 in the LHAR group (P=0.0436), and Duncaniella in the PCAR group (P=0.01) were significantly lower (Fig. 8c).

Impact of TCP on microbiota function in CTX-induced mice: By comparing the differences of MetaCyc metabolic pathways between different groups, the main metabolic pathways in CCAR group, MCAR group and PCAR group are shown in Fig. 9a. KEGG function analysis showed that the main metabolic pathways in CCAR group were *Glycosaminoglycan degradation, Streptomycin biosynthesis*, *Sphingolipid metabolism*, *Toluene degradation*, *Zeatin biosynthesis*, *Biosynthesis of siderophore group nonribosomal peptides, Alanine, aspartate* and *glutamate metabolism*, LHAR group were *Biosynthesis of ansamycins*, *beta-Lactam resistance* and *Plant-pathogen interaction*, PCAR group were *Bacterial chemotaxis*, *Two-component system* and *Lysine biosynthesis* (Fig. 9b). The results suggest that TCP may exert immunomodulatory effects by regulating the metabolic functions of microorganisms, but further experimental verification is needed.

Correlation analysis of intestinal flora and biochemical indicators: TCP decreased MDA and increased SOD & T-AOC→ Promoted antioxidant capacity. TCP increased IL-6, IL-1β, IL-10, and regulated TNF-α, supporting immune defense. TCP treatment reduced harmful gut microbiota and enhanced beneficial strains. TCP-shaped microbial metabolism impacting immune homeostasis and gut health. These observations established a significant association between the variation of gut microbiota composition and the improvement of relevant biochemistry with the treatment of TCP.

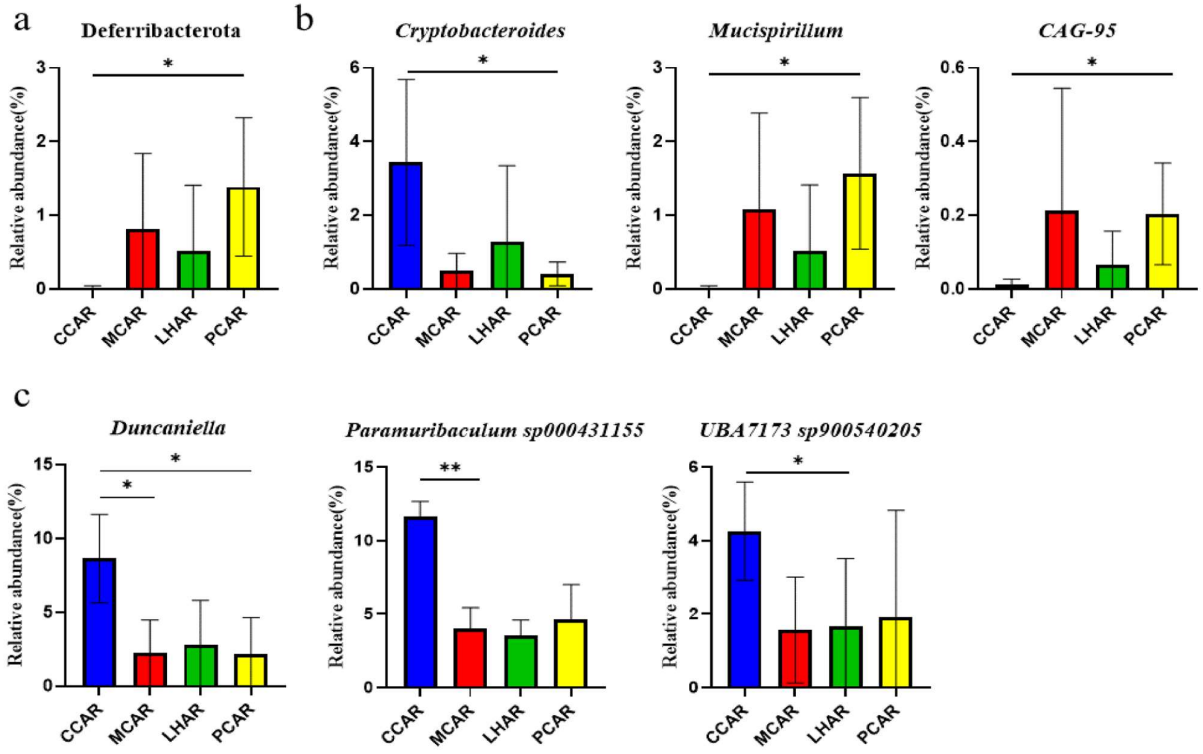

Fig. 8: Revealing the markedly different species between different mice via the T-test. *P<0.05; **P<0.01. a: Phylum, b: Genus, c: Species.

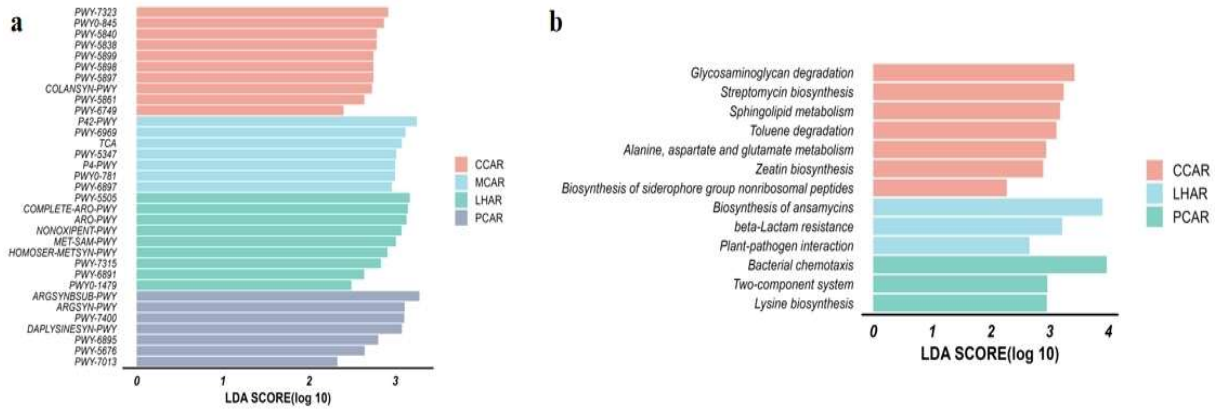

Fig. 9: Analyzing the microbiota function between CCAR, LHAR, PCAR, and MCAR. a: MetaCyc pathways of mice, b: KEGG pathways of mice.

DISCUSSION

Cyclophosphamide is a potent immunosuppressant known to induce immune-related disorders by compromising the mucosal barrier, weakening tight intestinal junctions, and promoting the activity of potentially pathogenic bacteria (Ahn *et al.,* 2008; Lee *et al.,* 2014). However, the relationship between *Tupistra chinensis* polysaccharide and gut microbes, as well as the specific regulatory mechanisms on immune function induced by CTX, remains unclear. To address this gap, we extracted polysaccharides from *Tupistra chinensis* and investigated their potential to alleviate CTX-induced immune dysfunction.

The spleen is a vital immune organ that plays a critical in mediating non-specific immune responses (Huang *et al.,* 2024); however, CTX has been reported to cause significant damage to its structure and function. Microscopic examinations revealed that the splenic tissue structure in the model group was severely destroyed, with unclear distinction between red and white pulp and a noticeable reduction in the number of *lymphocytes*, which indicated the vulnerability of immune organs and served as a clear indication of immunosuppression (Wu *et al.,* 2014; Khan *et al.,* 2022). Following TCP treatment, the splenic tissue appeared intact with a well-defined medulla margin, suggesting that TCP plays a significant role in preserving the normal function of immune organs. Comparison of the ileum and colon sections post treatment further revealed that TCP effectively alleviated CTX-induced inflammatory cell infiltration, intestinal epithelial cell injury, and collagen fiber hyperplasia, while maintaining intestinal structural integrity. Epithelial cells are not only critical in responding to pathogens but also transmit signals to the

intestinal immune system by releasing cytokines and inflammatory mediators (Kuhn *et al.,* 2014). TCP has been shown to support the intestinal immune system and immune organs by regulating the microbiota, stimulating cell proliferation, enhancing mucus production, thickening villi, and preserving epithelial connection and integrity (Liu *et al.,* 2019).

We conducted serum metabolomics analysis and observed that TCP influences serum cytokine levels as well as antioxidant and biochemical indices. Superoxide dismutase (SOD), a crucial antioxidant enzyme, plays a significant role in regulating levels of *reactive oxygen species* (Zhang *et al.,* 2020). MDA could form covalent bonds with proteins, nucleic acids, and other cellular molecules, which can lead to damage to cell functions and trigger inflammation. Its concentration is commonly regarded as an indicator of lipid peroxidation and oxidative stress (Chang *et al.,* 2017). T-AOC serves as an indicator of the body's antioxidant status, representing the overall level of antioxidants, which includes a variety of antioxidant substances and enzymes (Wang *et al.,* 2021). In the TCP treatment group, there was an increase in SOD and T-AOC levels, along with a decrease in MDA levels, suggesting that TCP effectively reduces oxidative damage in mice. Additionally, previous studies have reported that IL-1β is a proinflammatory cytokine with a variety of activities (Kirii *et al.,* 2003), IL-6 controls the development of chronic inflammatory diseases (Baran *et al.,* 2018), IL-10 is a recognized inflammatory and immunosuppressive factor (Gorby *et al.,* 2020), originally discovered for its anti-tumor activity, and TNF-α is one of the major inflammatory cytokines involved in initiating and spreading the inflammatory response (Chang *et al.,* 2017). The treatment with TCP resulted in increased levels of IL-1β, IL-6, IL-10, and TNF-α in the mice, suggesting that TCP effectively mitigates inflammation and modulates immune responses. These findings indicate that TCP has the potential to alleviate immune dysfunction induced by CTX. It is worth noting that although IL-10 is a classic anti-inflammatory cytokine, its level in the TCP treatment group was significantly higher than that in the model group, and it occurred simultaneously with the increase of pro-inflammatory factors IL-1β and IL-6. This phenomenon seems contradictory, but in the process of immune recovery, it precisely reflects the compensatory anti-inflammatory response. Under the immunosuppression induced by CTX, the basal level of IL-10 is decreased. The TCP treatment not only reactivated the pro-inflammatory immunity but also upregulated IL-10 as a feedback mechanism to prevent excessive tissue damage. Therefore, the increase of IL-10 in this study may be a physiological balance regulation rather than a transition to an anti-inflammatory state. Besides influencing gut structure, gut microbiota is crucial for maintaining gut health. Therefore, we proceeded to evaluate the diversity and composition of gut microbiota (Li *et al.,* 2021). The gut microbiota is a diverse microbial community that resides in the gastrointestinal tract and plays a vital role in maintaining the host's health (Schoeler *et al.,* 2019). Gut *dyshomeostasis* leads to dysbiosis in the gut microbiome, contributing to various diseases and abnormal immune responses. We conducted microbiome sequencing and obtained 1,862,003 filtered sequences. According to the α diversity index, the species abundance of mice in the TCP treatment group decreased compared to the model group, suggesting that TCP can eliminate harmful microorganisms that impair immune function. However, the abundance of mice in the TCP treatment group was slightly higher than that in the LH group, with more probiotic species, indicating a stronger effect than LH. TCP restored the microbiome disrupted by CTX and its function in mice.

Limosilactobacillus and *Ligilactobacillus* are intestinal probiotics, which can improve intestinal flora and enhance immunity (Li *et al.,* 2023). *Duncaniella* is a genus of opportunistic bacteria that causes infections (Miyake *et al.,* 2020), *Streptococcus* is also an opportunistic pathogen that can cause a variety of suppurative inflammation and hypersensitive diseases (Facklam *et al.,* 2002), *Dwaynesavagella* can invade the body through the respiratory tract or wounds, and is more common in immunocompromised individuals, such as cancer patients and in patients which are on long-term immunosuppressive drugs (Chang *et al.,* 2021), *Helicobacter_C_479931* is also an opportunistic pathogen that can cause infections (Tran *et al.,* 2005). In the MCAR group, which was treated only with CXT, the abundance of beneficial bacteria such as *Limosilactobacillus* and *Ligilactobacillus* was reduced, while pathogenic bacteria like *Duncaniella*, *Streptococcus*, *Dwaynesavagella*, and *Helicobacter_C_479931* were elevated. However, following TCP treatment, this imbalance was reversed, with an increase in probiotic bacteria and a reduction in harmful bacterial levels. The overall effect of TCP was comparable to the results observed with LH treatment. The findings suggest that TCP can mitigate immune function damage by enhancing the structure of the gut microbiota. This enhancement influences the abundance of metaCyc pathways and KEGG pathway functions, leading to an increase in immune factor anabolic pathways. Additionally, we investigated the marker species linked to TCP's effects on CTX-induced recovery in mice. Across the four groups of ICR mice, a total of seven genera showed significant differences. The relative abundance of the potential pathogenic bacterium Cryptobacteroides decreased, and this decrease was particularly significant in the PCAR group (Meucci *et al.,* 2015; Chen *et al.,* 2024). In conclusion, our study highlights the potential of *Tupistra chinensis* polysaccharides to alleviate CTX-induced immune dysfunction by reducing inflammation, enhancing antioxidant capacity, and regulating gut microbiota. *Tupistra chinensis* polysaccharide shows promising therapeutic effects. Future research should aim to further explore the mechanisms underlying its role in improving intestinal health. Additionally, Studies should explore its effects on immunomodulation and overall growth performance in livestock. These findings could contribute to developing therapeutic strategies for human health.

Conclusion: Tupistra chinensis polysaccharide has a restorative effect on CTX-induced immune dysfunction in mice by regulating oxidative stress and restoring the intestinal microbiome.

Author Contributions: QH, XW and TL carried out the conceptual and experimental work. QH, WL, HS and QD wrote the first draft of the manuscript. HA, MAA, WL, MMA, HS and QD contributed to the data analysis, writing

and review of the manuscript. HS and QD supervised the study. All authors have approved the manuscript for publication.

Data availability statement: Sequencing data used in this study were stored in the NCBI database under accession number: PRJNA1174412.

Ethics statement: All the experimental procedures were guided and approved by the Laboratory Animals Research Centre of Jiangsu, China, and the ethics committee of Nanjing Agricultural University (NJAU.No20220520108).

Conflict of Interest: No

REFERENCES

Ahlawat S, Kumar P, Mohan H, *et al.,* 2021. Inflammatory bowel disease: tri-directional relationship between microbiota, immune system, and intestinal epithelium. Critical Reviews in Microbiology 47:254-273.

Ahn G, Hwang I, Park E, *et al.,* 2008. Immunomodulatory effects of an enzymatic extract from Ecklonia cava on murine splenocytes. Marine Biotechnology 10:278-289.

Baran P, Hansen S, Waetzig GH, *et al.,* 2018. The balance of interleukin (IL)-6, IL-6 soluble IL-6 receptor (sIL-6R), and IL-6 sIL-6R sgp130 complexes allows simultaneous classic and trans-signaling. Journal of Biological Chemistry 293:6762-6775.

Biswas A, Petnicki-Ocwieja T and Kobayashi KS, 2012. Nod2: a key regulator linking microbiota to intestinal mucosal immunity. Journal of Molecular Medicine 90:15-24.

Cai YD, Liu YA, Wu ZF, *et al.,* 2023. Effects of diet and exercise on circadian rhythm: role of gut microbiota in immune and metabolic systems. Nutrients 5(12):2743.

Cascio MJ and Jen KY, 2018. Cocaine/levamisole-associated autoimmune syndrome: a disease of neutrophil-mediated autoimmunity. Current Opinion in Hematology 25:29-36.

Chang CS, Liao YC, Huang CT, *et al.,* 2021. Identification of a gut microbiota member that ameliorates DSS-induced colitis in intestinal barrier enhanced Dusp6-deficient mice. Cell Reports 37(8):110016.

Chang R, Yee KL and Sumbria RK, 2017. Tumor necrosis factor alpha inhibition for Alzheimer's disease. Journal of Central Nervous System Disease 9:1179573517709278.

Chen SA, Kang JX, Zhu HQ, *et al.,* 2024. Tea seed saponins ameliorate cyclophosphamide-induced intestinal injury, immune disorder and gut microbial dysbiosis in mice. Food Bioscience 57:103504.

de Jonge ME, Huitema ADR, Rodenhuis S, *et al.,* 2005. Clinical pharmacokinetics of cyclophosphamide. Clinical Pharmacokinetics 44:1135-1164.

Dong LN, Wang M, Guo J, *et al.,* 2019. Role of intestinal microbiota and metabolites in inflammatory bowel disease. Chinese Medical Journal 132:1610-1614.

Facklam R, 2002. What happened to the streptococci: overview of taxonomic and nomenclature changes. Clinical Microbiology Reviews 15:613-620.

Gorby C, Bellón JS, Wilmes S, *et al.,* 2020. Engineered IL-10 variants elicit potent immunomodulatory effects at low ligand doses. Science Signaling 13(649):eabc0653.

Han MM, Fan YK, Zhang Y, *et al.,* 2024. Advances in herbal polysaccharides-based nano-drug delivery systems for cancer immunotherapy. Journal of Drug Targeting 32:311-324.

Huang P, Jiang AQ, Wang XX, *et al.,* 2021. NMN maintains intestinal homeostasis by regulating the gut microbiota. Frontiers in Nutrition 8:714604.

Huang ZY, Sun KD, Luo ZY, *et al.,* 2024. Spleen-targeted delivery systems and strategies for spleen-related diseases. Journal of Controlled Release 370:773-797.

Kara O, 2024. Protective effect of coenzyme Q10 in cyclophosphamide-induced kidney damage in rats. Revista da Associacao Medica Brasileira 70(4):e20230990.

Khan AI, Rehman AU, Farooqui NA, *et al.,* 2022. Effects of shrimp peptide hydrolysate on intestinal microbiota restoration and immune modulation in cyclophosphamide-treated mice. Molecules 27(5):1720.

Kirii H, Niwa T, Yamada Y, *et al.,* 2003. Lack of interleukin-1β decreases the severity of atherosclerosis in ApoE-deficient mice. Arteriosclerosis Thrombosis and Vascular Biology 23:656-660.

Kuhn KA, Pedraza I and Demoruelle MK, 2014. Mucosal immune responses to microbiota in the development of autoimmune disease. Rheumatic Disease Clinics of North America 40:711-720.

Lee JK, Jeon JK and Byun HG, 2014. Antihypertensive effect of novel angiotensin I converting enzyme inhibitory peptide from chum salmon skin in spontaneously hypertensive rats. Journal of Functional Foods 7:381-389.

Li JJ, Feng SF, Wang ZY, *et al.,* 2023. *Limosilactobacillus mucosae*-derived extracellular vesicles modulate macrophage phenotype and orchestrates gut homeostasis in a diarrheal piglet model. NPJ Biofilms and Microbiomes 9:33.

Li X, Wu D, Niu JJ, *et al.,* 2021. Intestinal flora: a pivotal role in investigation of traditional Chinese medicine. American Journal of Chinese Medicine 49:237-268.

Li X, Xu C, Chen J, *et al.,* 2024. Effect of *Tupistra chinensis* baker therapy on intestinal injury induced by Escherichia coli. Pakistan Veterinary Journal 44:1033-1042.

Liang X, Chen J, Xu C, *et al.,* 2025. *Tupistra chinensis* polysaccharide mitigates the inflammatory response by regulating gut-microbiota in mice induced by LPS. Pakistan Veterinary Journal 45(3):1353-1360.

Lin Y, Lourenco JM and Olukosi OA, 2023. Effects of protease, xylanase and xylo-oligosaccharides on growth performance and microbiota in broiler chickens. Poultry Science 102(8):102789.

Liu X, Zhang ZJ, Liu JH, *et al.,* 2019. Ginsenoside Rg3 improves cyclophosphamide-induced immunocompetence in mice. International Immunopharmacology 72:98-111.

Meng A, Zhang X, Pubu P, *et al.,* 2024. Protective effect of lentinan against LPS-induced injury in mice via antioxidant and microbiota regulation. Pakistan Veterinary Journal 44:647-656.

Meucci A, Zago M, Rossetti L, *et al.,* 2015. *Lactococcus hircilactis* sp. nov. and *Lactococcus laudensis* sp. nov. isolated from milk. International Journal of Systematic and Evolutionary Microbiology 65:2091-2096.

Miyake S, Ding YC, Soh M, *et al.,* 2020. Cultivation and description of Duncaniella species. International Journal of Systematic and Evolutionary Microbiology 70:3105-3110.

Nguyen DH, Ta NAT, Van HG, *et al.,* 2024. Effects of probiotic LabMix on immune indices and microbiota. Asian Journal of Agriculture and Biology 2024:2023241.

Pan WB, Chang FR and Wu YC, 2000. *Spirostanol sapogenins* from *Tupistra chinensis*. Chemical and Pharmaceutical Bulletin 48:1350-1353.

Pan ZH, Li Y, Liu JL, *et al.,* 2012. Cytotoxic compounds from *Tupistra chinensis*. Fitoterapia 83:1489-1493.

Peng S, Xu C, He Q, *et al.,* 2024. Fucoidan alleviates intestine damage via microbiota regulation. Pakistan Veterinary Journal 44:517-525.

Ponticelli C and Glassock RJ, 2019. Prevention of complications from immunosuppressants. Journal of Nephrology 32:851-870.

Schoeler M and Caesar R, 2019. Dietary lipids, gut microbiota and metabolism. Reviews in Endocrine and Metabolic Disorders 20:461-472.

Shim JO, 2013. Gut microbiota in inflammatory bowel disease. Pediatric Gastroenterology Hepatology and Nutrition 16:17-21.

Tran CD, Campbell MAF, Kolev Y, *et al.,* 2005. Zinc supplementation attenuates gastritis. Journal of Infection 50:417-424.

Virili C, Stramazzo I and Centanni M, 2021. Gut microbiome and thyroid autoimmunity. Best Practice and Research Clinical Endocrinology and Metabolism 35(3):101506.

Wang MY, Zhang SF, Zhong RQ, *et al.,* 2021. Olive fruit extracts improve antioxidant capacity via microbiota. Frontiers in Nutrition 8:645099.

Wang N, Xiang Y, Ma Y, *et al.,* 2024. Fermented Spirulina alleviates ulcerative colitis via gut microbiota regulation. Asian Journal of Agriculture and Biology 2024(1):2023232.

Wei LM, Wu YC, Chen CC, *et al.,* 2014. Tupichinins B-D from *Tupistra chinensis*. Natural Product Research 28:74-80.

Wu XF, Fan JJ, Ouyang ZJ, *et al.,* 2014. *Tupistra chinensis* extract attenuates hepatitis. Journal of Pharmacy and Pharmacology 66:453-465.

Xiao YH, Zhang GJ, Zong L, *et al.,* 2019. Chemical constituents and antitumor activity of *Tupistra chinensis.* Chemical Journal of Chinese Universities 40:1897-1903.

Xu C, He Q, Zhu Z, *et al.,* 2025. Propolis improves intestinal barrier function against Cryptosporidium parvum via NLRP6 inflammasome. mBio 16(11):e0231725.

Xu Y, Liang XF, Li YZ, *et al.,* 2020. Arylsulfonamides from *Tupistra chinensis*. Natural Product Communications 15(4):1-5.

Yi XM, Xiang LM, Huang YY, *et al.,* 2018. Apoptosis induced by saponin from *Tupistra chinensis*. Phytomedicine 42:83-89.

Ying Y and Hao W, 2023. Immunomodulatory function of natural polysaccharides. Frontiers in Immunology 14:1147641.

Zhang YX, Li T, Yuan HQ, *et al.,* 2018. Correlations of inflammatory factors with intestinal flora. Medical Science Monitor 24:7975-7979.

Zhang R, Wang L, Zhao QH, *et al.,* 2020. Extracellular superoxide dismutase in pulmonary hypertension. Frontiers in Medicine 7:509.

Zhao Q, Wang J, Liang H, *et al.,* 2024. Prevention of cyclophosphamide-induced immune suppression by polysaccharides from *Apocynum venetum* flowers *via* enhancing immune response, reducing oxidative stress, and regulating gut microbiota in mice. Frontiers in Pharmacology 15:1354794.

Zheng HT, Zhao QY, Ding Y, *et al.,* 2023. RSV infection and intestinal flora. European Review for Medical and Pharmacological Sciences 27:2671-2678.